Proceedings of the 11th Brazilian Congress of Thermal Sciences and Engineering -- ENCIT 2006
Braz. Soc. of Mechanical Sciences and Engineering -- ABCM, Curitiba, Brazil,- Dec. 5-8, 2006

Paper CIT06-0546

Wing and Airfoil Optimized Design of Transport Aircraft

J Allan Antunes Lyrio
Technological Institute of Aeronautics (ITA) – São José dos Campos – SP - Brazil
j.antunes@embraer.com.br

Juliano Machado Tenório Cavalcanti
Technological Institute of Aeronautics (ITA) – São José dos Campos – SP - Brazil
Juliano.cavalcanti@embraer.com.br

Bento Silva de Mattos
Technological Institute of Aeronautics (ITA) – São José dos Campos – SP - Brazil
bmattos@ita.br

Nide G. C. R. Fico Junior
Technological Institute of Aeronautics (ITA) – São José dos Campos – SP - Brazil
nide@ita.br

Pedro Paglione
Technological Institute of Aeronautics (ITA) – São José dos Campos – SP - Brazil
paglione@ita.br

Abstract. *An efficient methodology for multi-disciplinary design and optimization of transport was elaborated and developed. The methodology was implemented in a commercial known optimization framework. Semi-empirical methods were employed for wing weight estimation; a multi-block full-potential code was used for drag calculation; Vortex Lattice method was implemented for spanwise lift distribution in order to compute de aircraft maximum-lift coefficient via critical section method; a calibrated single-point Breguet simplified equation was considered for aircraft performance calculation. The optimization design variables are related to the wing planform and airfoil geometry and cruise speed. The design constraints were the fuel tank capacity, flight quality of the aircraft, and takeoff field length. A simple stability augmentation control system was implemented in order to compute its effects on optimal configurations. Multi-objective optimization tasks were performed accomplishing minimization of the block time and block fuel for a specified mission.*

Keywords *Aircraft Design, Multi-Disciplinary Design and Optimization, Evolutionary Algorithms, Wing Design*

1. Symbols and Abbreviations

MDO	=	Multi-disciplinary design and optimization
FPWB	=	Refers to a Full-potential Wing Body code
$L_{1\text{-}LE}$	=	Distance between the first spar and the wing leading edge at the break station
$L_{23\text{-}TE}$	=	Distance between the secondary or auxiliary spar and the wing trailing edge at the break station
AR_w	=	Wing aspect ratio
λ_i	=	Inner wing taper
λ_o	=	Outer wing taper
Y_K	=	break station location coordinate along wingspan
Λ_{LEi}	=	Leading-edge sweep angle of the inner wing
Λ_{LEo}	=	Leading-edge sweep angle of the outer wing
S_w	=	Wing reference area
W_p	=	Wing position at the fuselage
V_{HT}	=	Horizontal tail volume
W_w	=	Wing weight
K_T, K_R	=	Weight estimation calibration factors
S_{ctr}	=	Wing controls surface area
n_{ult}	=	Ultimate load factor
b_w	=	Wingspan
MTOW	=	Maximum takeoff weight
MZFW	=	Maximum zero-fuel weight
MUFW	=	Maximum usable-fuel weight
λ	=	Equivalent wing taper

$(t/c)_{avg}$ = Average thickness of the wing
$(t/c)_r$ = Maximum thickness @ wing-fuselage junction
$\Lambda_{1/4}$ = Equivalent wing quarter-chord sweep
HT = Abbreviation for horizontal tail
CG = Center of gravity
MLG = Main landing gear
CFD = Computational fluid dynamics
AOA = Angle of attack
S_{HT} = Area of the horizontal empennage
Cl(y) = Section lift coefficient
$Cl_0(y)$ = Section zero-lift coefficient
$Cl_3(y)$ = Section lift coefficient @ three degrees angle of attack
$Cl_a(y)$ = Section lift slope
SAS = Stability augmentation system
DOC = Direct Operating Cost
V2 = Takeoff safety speed. Also called takeoff screen speed, the minimum speed in the second segment of a climb following an engine failure.

2. Introduction

There is a need for a software infrastructure in aircraft design that facilitates collaboration and data sharing, while providing comprehensive data management capabilities in line with modern information technologies standards[9]. The present work addresses some issues in that direction. It is concerned with optimal aircraft design. In this context, an efficient framework was built up for the conceptual design of transport aircraft. Since the early 60´s MDO has been a motivation of study for a great number of researches[1,2], However, only with the advent of high-speed computing, its true benefit could be useful to the aeronautical industry. MDO has been at the spotlight of the industry for the last 15 years but its heavy application in the aeronautical industry only started in the last five years. This can be explained by the high complexity of the aeronautical design, and the low automation at all levels of design. Since the 80´s several authors have described numerous techniques on aircraft design[4,5,6]. In 2001, Kroo[2] described several aeronautical process formulations and commented on some process integration. Askin[1], in his 2002 Ph.D. thesis, besides applying MDO for aircraft design, also describes and even intrudes some methodology for aircraft design. Versiani et all[3], in 2004, conducted some aircraft configuration optimization with genetic algorithm for a business jet considering a variant carrying a larger payload with a small range penalty. In his work, the optimization tasks were performed with aircraft fitted with trapezoidal wings only. Cavalcanti et all[11] conducted optimization tasks for complex configurations with fixed airfoil geometry. Besides the more complex wing planform layouts the present considers airfoil geometry variation along optimization. Among other features, it was taken into account feasible structural layout also able to accommodate the main landing gear. A lot of effort was put for the validation of routines to compute configuration parameters such as overall weight of the configuration or of its parts. This was needed in order to evaluate aircraft performance. ESTECO® - modeFrontier package was employed as optimization framework for the present methodology. modeFrontier is a multi-objective optimization and design environment that allow easy coupling to almost any computer aided engineering (CAE) tool.

3. Optimization framework

The MDO workflow considers three areas in the optimization process: aerodynamics, stability and control, weight and balance and performance. A module for configuration management is also part of the framework. This module generates all the necessary data required by the remained ones. The calculation of maximum capacity of the fuel tank is also performed by the geometry management module, which will be appropriately described in next section. **Figure 1** presents the MDO workflow of the present work.

3.1 Geometry management module

The module for the construction of the typical wing planform provides all the required geometric data required for calculations performed by other modules. It was implemented in Microsoft® - Excel software, and a typical wing layout generated with this tool can be seen in **Figure 2**. The structural wing layout is comprised of two main spars and an auxiliary one for the attachment of the main landing gear. Areas of control surfaces as well as that of the high-lift system are also computed in this module. The module also performs some checks concerning the feasibility of the general wing layout.

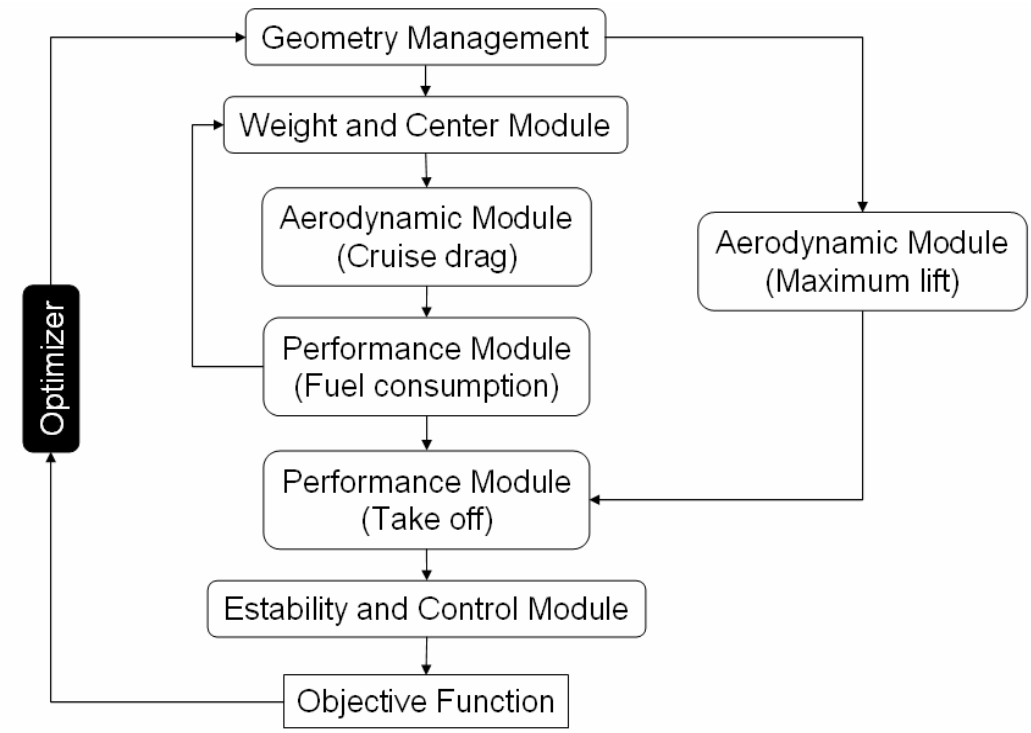

Figure 1 - MDO Workflow.

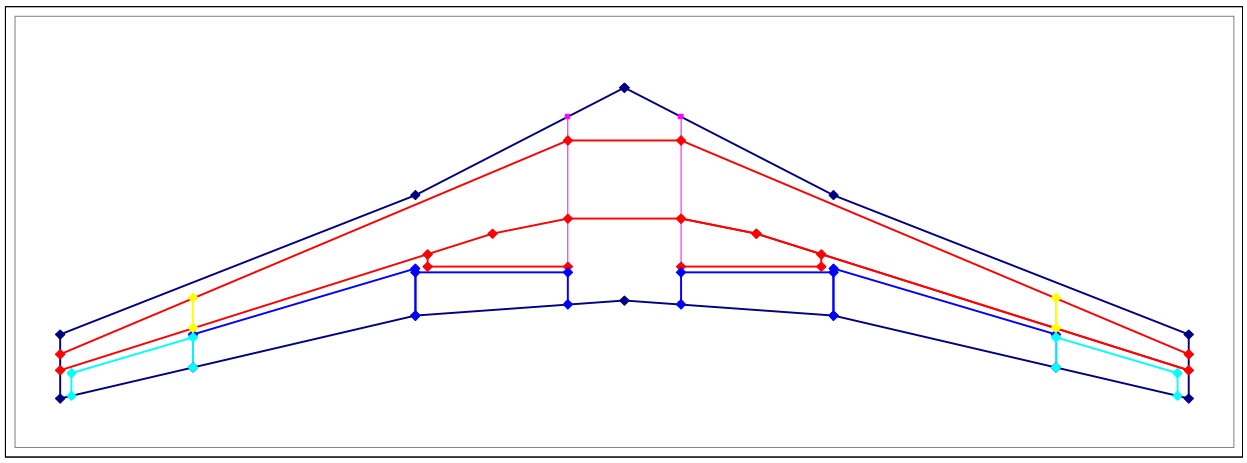

Figure 2 - Wing planform and structural layout generated by the configuration management module.

The input variables for the optimization of the wing planform are listed in **Table I** with their respective lower and upper boundaries. The variables values are allowed to change according to engineering expertise, and must be restrained in order to generate a feasible configuration. In **Figure 2**, it can be seen that the spar location must be taken as optimization variable in order to achieve a compromise among the inertia of the wingbox, volume of the fuel tank and, and areas of flaps and ailerons.

The semi-empirical method adopted in the present work does not require the spars and ribs layout for the weight estimation. For this reason, the inertia of the wingbox is not calculated. Thus, the spar layout is not considered as optimization variable and therefore it will be kept constant relative to the root and tip wing chords.

The geometry management module allows for checking the wing physical construction feasibility. This is performed by measuring the following distances at the kink spanwise station: between the front spar and the leading edge, L_{1-LE} ; form the trailing edge to the auxiliary or secondary spar, L_{23-TE} , depending on the kink station location. When these distance becomes negative, i.e, when the spars cross the leading or trailing edges of the wing, representing a non-feasible solution, the fuel tank volume is calculated as zero and the maximum fuel tank capacity constraint will penalize this experiment.

Variable	Short description	Lower boundary	Upper boundary
AR_w	Aspect ratio	6	11
λ_i	Taper ratio of inner wing	0.5	0.8
λ_o	Taper ratio of outer wing	0.1	0.5
Y_K	Location of the break station	0.3	0.4
Λ_{LE_i}	Leading-edge sweep angle of inner wing	15º	35º
Λ_{LE_o}	Leading-edge sweep angle of outer wing	15º	35º
S_w	Reference area	80 m^2	150 m^2
W_p	Wing position relative to fuselage	40 %	50 %
V_H	Volume coefficient of the horizontal tail	0.8	1.5

Table I – Geometric variables for the optimization process.

The module for the management of the aircraft configuration also calculates the so called reference – equivalent - wing. The equivalent wing is a method which attempts to transform a cranked wing into a trapezoidal one, simplifying numerous geometrical based analyses. There are several equivalent wing generation methods. Askin[1] proposed the ESDU equivalent wing method for wings with non-constant leading edge sweep. The basic principles of this method are show at **Figure 3**.

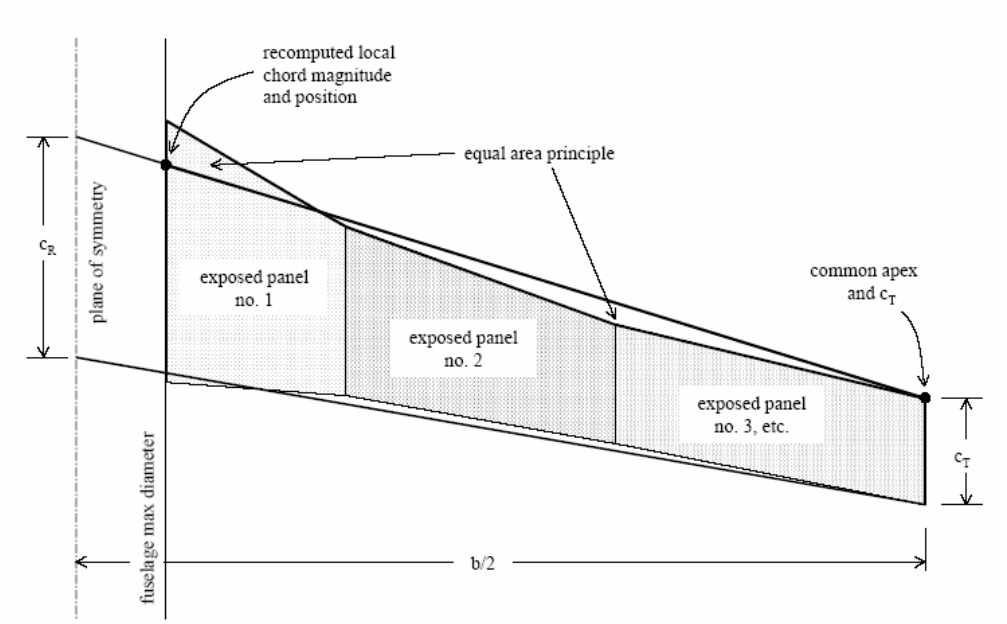

Figure 3 - ESDU definition for reference wing.

Due to CFD analisys implemented at the aerodynamic calculations, which can compute more complexes wing layout, the usefulness of equivalent wing was restricted to the weight estimation only - described in the following section.

The airfoil lofting was parameterized with polynomials[12], which provide the thickness and camber curves.

$$y_t = a_1\sqrt{x} + a_2 x + a_3 x^2 + a_4 x^3 + a_5 x^4 \tag{1}$$

$$y_c = b_1 x + b_2 x^2 + b_3 x^3 + b_4 x^4 + b_5 x^5 + b_6 x^6 \tag{2}$$

The values for the coefficients of the polynomials in **Eqs. (1)** and **(2)** are obtained from the 11 characteristics variables for three spanwise stations (root, break and tip wing locations). The parameterization method is able in providing a very concise description of supercritical airfoils. After planform and airfoils definitions, the wing surface topology is built by airfoils linear interpolations (**Figure 4).**

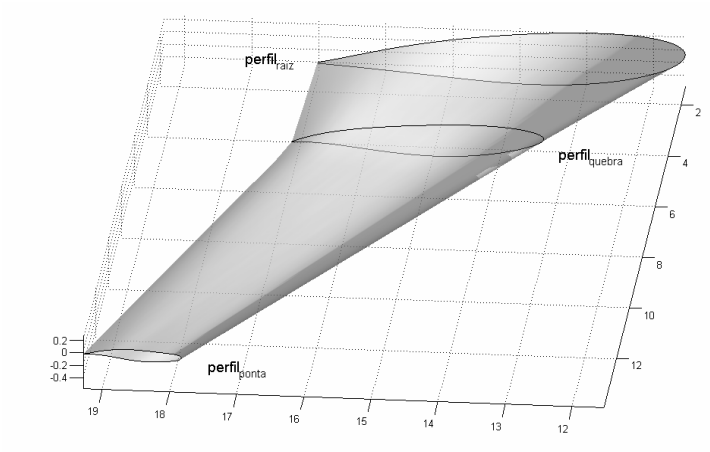

Figure 4 – Typical transport aircraft wing defined by three airfoil geometries.

3.2 Weight and Balance Module

This module performs the estimation of the wing weight and the calculation of the momentum of inertia. The wing weight estimation is based at Torenbeek[4] and Raymer[5] semi-empirical formulation described at **Eq. 1** and **2.**

$$W_{w_T} = K_T \cdot 0.0017 \cdot MZFW \cdot \left(\frac{b_w}{\cos\left(\Lambda_{1/4}\right)} \right)^{0,75} \cdot \left(1 + \left(6.3 \cdot \frac{\cos\left(\Lambda_{1/4}\right)}{b_w} \right)^{0,5} \right) \cdot \cdot n_{ult}^{\,0,55} \cdot \left(\frac{b_w \cdot S_w}{\left(t/c\right)_{avg} \cdot MZFW \cdot \cos\left(\Lambda_{1/4}\right)} \right)^{0,3} \tag{3}$$

$$W_{w_R} = K_R \cdot 0.0051 \cdot \left(MTOW \cdot n_{ult}\right)^{0.557} \cdot S_w^{\,0.649} \cdot AR_w^{\,0.5} \cdot \left(t/c\right)_r^{-0.4} \cdot \left(1+\lambda\right)^{0.1} \cdot \cdot \cos\left(\Lambda_{1/4}\right)^{-1} \cdot S_{ctr}^{\,0.1} \tag{4}$$

Eq. 1 and **2** are in English units, and K_T and K_R are Torenbeek and Raymer methodology calibration factors, respectively. These factors were calibrated in the present work for aircraft listed in **II**. The parameter n_{ult} is the ultimate load factor, from which was proposed by Askin a value of 3.75 for jet transport aircraft; S_{ctr} is the wing controls surface area; b_w is the span of the wing; $MZFW$ and $MTOW$ are the maximum zero-fuel and maximum take off weight, respectively; $(t/c)_{avg}$ and $(t/c)_r$ are the average airfoil thickness and the thickness of the wing section at the junction to the fuselage. $\Lambda_{1/4}$ is the symbol for the quarter-chord sweep of the reference wing; λ is the taper ratio of the reference wing.

Method	Embraer 170	Embraer 190
Raymer	1 %	-1 %
Torenbeek	-1 %	1 %

Table II – Errors of the wing weight from the method adopted in the present work.

Therefore, the wing weight calculation in the present work will be carried out according to **Eq. 3**.

$$W_W = \frac{W_{W_T} + W_{W_R}}{2} \tag{5}$$

It can be noticed from **Eq. 3** and **4** that the maximum takeoff and the maximum zero-fuel weight (MTOW and MZFW) must be known in order to estimate the wing weight. However, for MTOW calculation, the wing weight must be added to the so called fixed weight (fuselage, empennage, payload and all other aircraft parts that will be constant during optimization) and to the fuel weight. This implies that an iterative solution is in place, considering that the wing and fuel weight can not be determined until weight and performance modules finalize their calculations, respectively. **Figure 5** show schematics on how this iteration is implemented at the workflow.

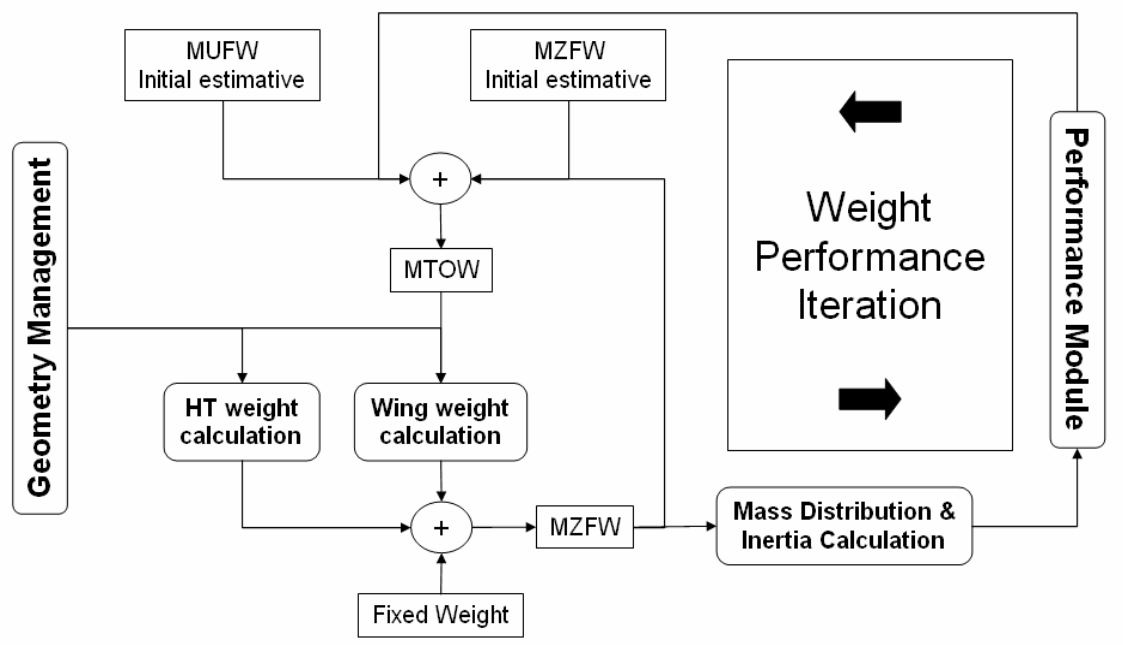

Figure 5 - MZFW and required fuel calculation.

It can be seen from **Figure 5** that the weight calculation of the HT is also needed for the MZFW prediction. However, since only horizontal tail volume will be changed, hence, only its area, no semi-empirical method will be used, and the HT weight will be considered as changing proportionally with its area. This hypothesis can be emphasized considering that no additional parameter at the HT will be changed, such as aspect ratio or sweep.

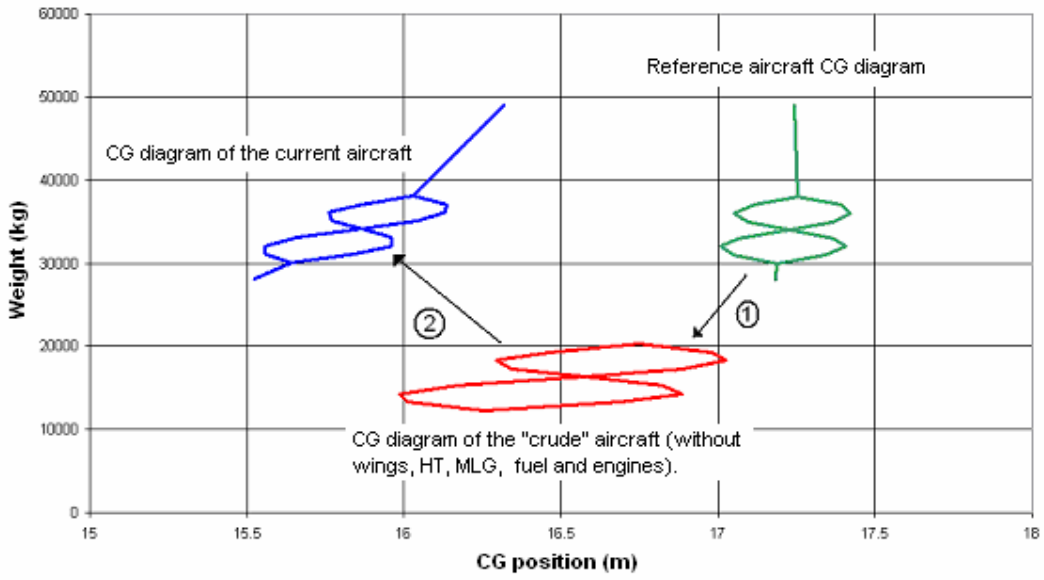

Figure 6 - CG diagram.

As can be seen from **Figure 5**, the weight and balance module also performs the mass distribution and inertia calculation of the aircraft. That is necessary for the stability and control module, which needs forward and aft CG position of the aircraft and their respective inertia. The CG position, in middle of cruise is another important calculation because it is required to calculate the aerodynamic forces acting on the wing and HT. This is performed by considering a CG diagram of a reference aircraft, then the components subjected to weight and position modification are moved out and then these new components are placed at the current aircraft with their new values of weight and position, as show in **Figure 6**.

3.3 Aerodynamic calculation at cruise

The aerodynamic modules described in **Figure 1**, performs different tasks along the optimization process. The cruise aerodynamic module computes the aircraft drag at a given lift coefficient. This lift coefficient is computed considering the medium cruise weight, calculated at the weight module. Since in the present work the block-time is considered as an objective to be minimized, the cruise Mach number is considered as an independent design variable, with upper and lower limits of 0.75 and 0.85, respectively. Considering the design variables of **Table I**, the present work takes into account 10 design variables.

In order to compute the lifting force at the wing and HT, a calculation for trimmed aircraft is performed. The drag for the wing and HT are calculated separately. The drag part due to wing is calculated by using a full-potential code with boundary layer correction for lifting surfaces. The code is only able to perform calculations for wing-body configurations. A typical multi-block mesh result can been seen in **Figure 7**. The drag from the horizontal tail is obtained using classical aerodynamic formulation for drag calculation.

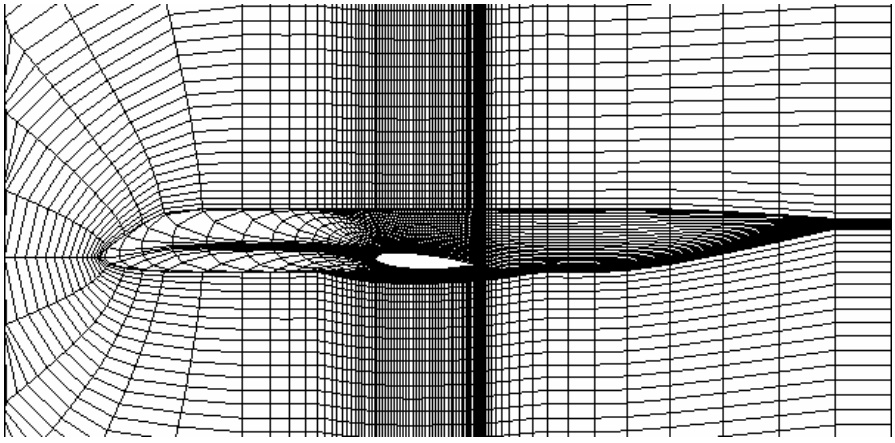

Figure 7- Cut view of a typical mesh for the full-potential code employed in the present work.

3.4 Maximum Lift Coefficient Calculation

The wing maximum lift calculations was estimated by Critical Section Method, that using a Vortex Lattice formulation for computing the spanwise lift distribution and 2-D data[13] for airfoil maximum lift coefficient. Once the maximum lift coefficient for sections is calculated, the wing maximum lift distribution can be obtained for comparison between span wise distribution and airfoils maximum lift. **Figure 8** shows a scheme for the calculation of the minimum distance between the spanwise lift distribution and the section maximum coefficient.

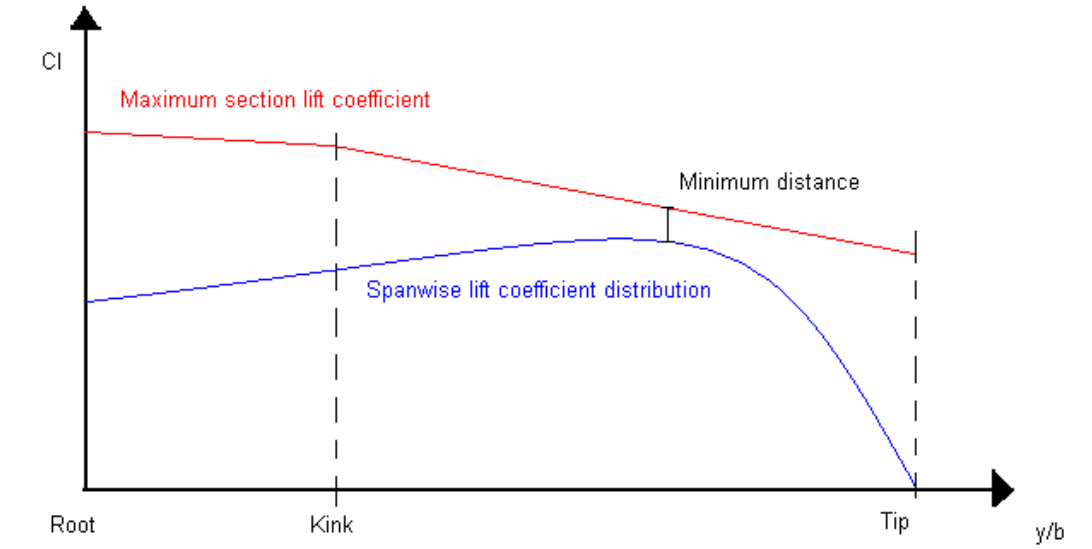

Figure 8. Critical section method for C_{Lmax} calculation.

Once the minimum distance expressed at **Figure 8** is know, a Mathworks® - MatLab script was developed, which attempts to minimize this by changing the wing AOA. So, the wing stall is considered to begin when the spanwise lift coefficient distribution intersects its respective maximum section lift coefficient. This methodology is considered a conservative one, since real wings can slightly increase its lift even if some spanwise sections are already stalled.

3.4 Stability and Control Module

The stability and control module will perform calculations in order to verify the aircraft flight quality. It will also check the controllability of the aircraft by computing the deflection of the HT at the approach flight phase. The implemented stability calculation is simplified formulation proposed by Nelson[7] and this is based on the so called dimensional derivatives. **Table III** contains a summary of the dimensional derivatives related to the longitudinal short-period dynamic mode.

$$Z_\alpha = C_{Z_\alpha} \frac{q \cdot S_w}{W} \qquad M_q = C_{m_q} \frac{\bar{c}}{2 \cdot u_0} \frac{q \cdot S_w \cdot \bar{c}}{I_{yy}} \tag{6}$$

$$M_\alpha = C_{m_\alpha} \frac{q \cdot S_w \cdot \bar{c}}{I_{yy}} \qquad M_{\dot{\alpha}} = C_{m_{\dot{\alpha}}} \frac{\bar{c}}{2 \cdot u_0} \frac{q \cdot S_w \cdot \bar{c}}{I_{yy}} \tag{7}$$

Table III - Longitudinal short-period dimensional derivatives.

The stability derivatives presented in **III** were calculated using the expressions presented in **Table IV** and the aerodynamics derivatives presented in **Table IV** were calculated using the full potential code when related to the wing, and the so called Vortex-Lattice, an aerodynamic code for subsonic calculation, when related to the HT.

$$C_{Z_\alpha} = -\left(C_{L_{\alpha_{wf}}} + C_{L_{\alpha_{HT}}} \frac{S_{HT}}{S_w} \left(1 - d\varepsilon / d\alpha\right) \right) \tag{8}$$

$$C_{m_q} = \left(-2 \cdot C_{L_{\alpha_{HT}}} \cdot \eta \cdot V_H \frac{l_{HT}}{\bar{c}} \right) \cdot 1{,}1 \tag{9}$$

$$C_{m_\alpha} = C_{L_{\alpha_{wf}}} \left(\bar{X}_{CG} - \bar{X}_{AC_{wf}} \right) + C_{L_{\alpha_{HT}}} \cdot \eta \cdot \left(1 - d\varepsilon / d\alpha\right) \cdot \left(\bar{X}_{CG} - \bar{X}_{AC_{HT}} \right) \frac{S_{HT}}{S_w} \tag{10}$$

$$C_{m_{\dot{\alpha}}} = -2 \cdot C_{L_{\alpha_{HT}}} \cdot \eta \cdot V_{HT} \frac{l_{HT}}{\bar{c}} \cdot \frac{d\varepsilon}{d\alpha} \tag{11}$$

Table IV - Longitudinal stability derivatives summary.

It is also necessary to compute the controls derivatives and the dimensional controls derivatives, expressed in **Tables V** and **VI**.

$$C_{Z_{\delta_e}} = -C_{L_{\alpha_{HT}}} \cdot \tau \cdot \eta \cdot S_{HT} / S_w \tag{12}$$

$$C_{m_{\delta_e}} = -C_{L_{\alpha_{HT}}} \cdot \tau \cdot \eta \cdot V_H \tag{13}$$

Table V - Control derivatives.

$$Z_{\delta_e} = C_{Z_{\delta_e}} \frac{q \cdot S_w}{W} \quad (14a) \qquad M_{\delta_e} = C_{m_{\delta_e}} \frac{q \cdot S_w \cdot \bar{c}}{I_{yy}} \quad (14b)$$

Table VI - Control dimensional derivatives.

The parameter τ is the so called flap effectiveness parameter, and can be computed as a function of the elevator to HT ratio, as show in **Figure 9**.

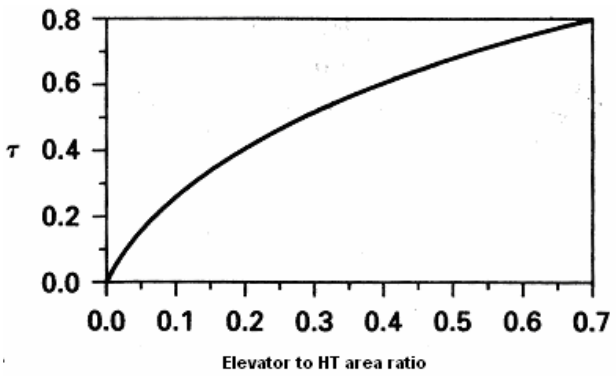

Figure 9 - Flap effectiveness parameter.

Provided all dimensional derivatives are calculated, Nelson[7] demonstrated that the state-space of the short-period system dynamics can be expressed as show in **Eq. 15**.

$$\begin{bmatrix}\dot{\alpha}\\ \dot{q}\end{bmatrix} = \underbrace{\begin{bmatrix} Z_\alpha/u & 1 \\ \left(M_\alpha + M_{\dot{\alpha}} \cdot Z_\alpha/u\right) & \left(M_q + M_{\dot{\alpha}}\right)\end{bmatrix}}_{A} \underbrace{\begin{bmatrix}\alpha\\ q\end{bmatrix}}_{X} + \underbrace{\begin{bmatrix} Z_{\delta_e}/u \\ M_{\delta_e} + M_{\dot{\alpha}} \cdot Z_{\delta_e}/u\end{bmatrix}}_{B} \cdot \left[\delta_e\right] \qquad (15)$$

By obtaining the eigen values of the matrix A, it is possible to obtain the natural frequency and damping ratio of the short-period mode. Providing these two parameters are calculated, the aircraft flight quality can then be analyzed using the graph shown in **Figure 10**.

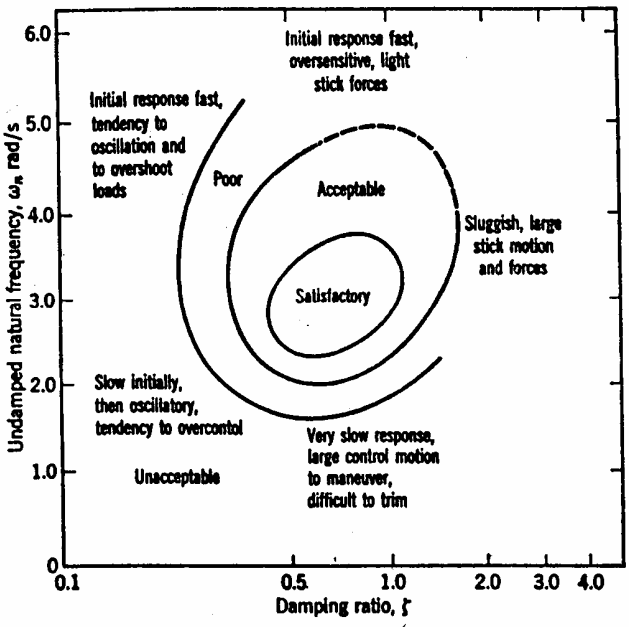

Figure 10 - flight quality diagram for the short-period behavior.

After analyzing the aircraft flight quality in the so called direct mode, i.e, without any stability augmentation system (SAS) in action, a simple SAS can be implemented to evaluation of some the benefits from its application. The implemented SAS has a simple architecture and works with the feedback of the aircraft AOA and the pitch rate, as shown in **Figure 11**.

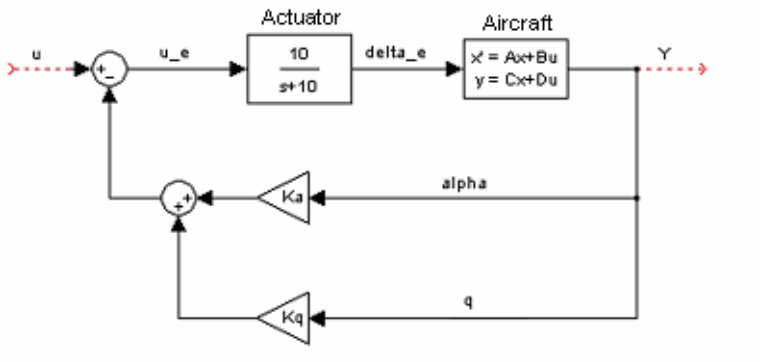

Figure 11- SAS architecture.

The SAS control logic was implemented with MatLab®, and its main task is to improve the closed loop system dynamics in order that its natural frequency and damping ratio be located in the center of the region relative to the satisfactory flight quality (**Figure 10**), by changing the values of the AOA and pitch rate gains. The desired natural frequency and damping ratio was set at the SAS to be 3 rad/s and 0.7 respectively.

The flight quality analysis were performed for two different flight phases, classified in level B and C, related to the cruise stage and the last to the approach stage, respectively.

3.5 Performance Module

The performance module uses the cruise aerodynamic module information to perform the block-fuel calculation for a mission of 2511 nm @ 37,000 ft with a payload of 6890 kg. The block-time is calculated based at the cruise Mach number, hence the climb and descent time are not being considered in the current analysis. Precisely 1600 kg fuel reserves for a 100 nm alternative and a 45 minutes holding have to be taken into account and were considered for all designs. Aircraft specific range, *SR* can be calculated as show in **Eq. 16**.

$$SR = M \cdot \frac{L}{D} \cdot \frac{1}{SFC(M)} \tag{16}$$

In **Eq. 16**, the Mach number is a design variable, the lift to drag ratio is considered at being at the mean value at the cruise flight phase, and provided by the aerodynamic module, and the *SFC(M)* is the engine specific fuel consumption. Since at the current analysis the engine is considered the same for all designs, the *SFC* will be the same. However, it is a function of the cruise Mach number and the cruise flight level. Once the cruise flight level is also considered as being constant, the engine *SFC* was predicted by a simple polynomial interpolation, as a function of the Mach number, as showed at **Eq. 16**. Once the aircraft *SR* is calculated, the block-fuel can be computed simply multiplying the *SR* by the cruise range, as seen on **Eq. 17**.

$$blkf = k_1 \cdot SR \cdot range \tag{17}$$

In **Eq. 17**, k_1 is a calibration factor which attempts to compute the take-off, climb and descent segments in the simple formulation described by **Eq. 17**.

The takeoff field length calculation is carried out according to the methodology described in reference [8], which is a variation of the *Take off Parameter* method. It is beyond the scope of this work to provide details regarding the fundaments of the ref. [8] method.

The parameters necessary for the calculation of the takeoff distance are

- Aircraft MTOW
- Aircraft maximum lift coefficient
- Wing area
- Engine settings at takeoff
- Aircraft lift and drag at V2.

4. Requirements for the optimization task

This section presents a brief summary of the optimization main requirements described at **Section 3**. The proposed optimization can not differs from any other optimization process. This indicates that three main topics must be clearly highlighted in the present work: optimization variables, objective functions, and constraints.

In order to compute de performance improvement due to optimization a generic aircraft were created in which the design variables were based on aircrafts from the same category already on the market. **Table VII** presents the chosen design planform variables and **Figure 12** shows the chosen airfoil sections for the reference aircraft, and **Table VIII** the baseline aircraft behavior according to the prescribed formulation.

Wing aspect ratio	8.5
Inner Wing taper ratio	0.65
Outer wing taper ratio	0.4
Break station location	0.35
Wing inner leading edge sweep	25º
Wing outer leading edge sweep	25º
Wing reference area	95 m^2
Cruise Mach number	0.78
Wing position (% fuselage)	45 %
HT volume coefficient	1.2

Table VII - Planform design variables for the baseline configuration.

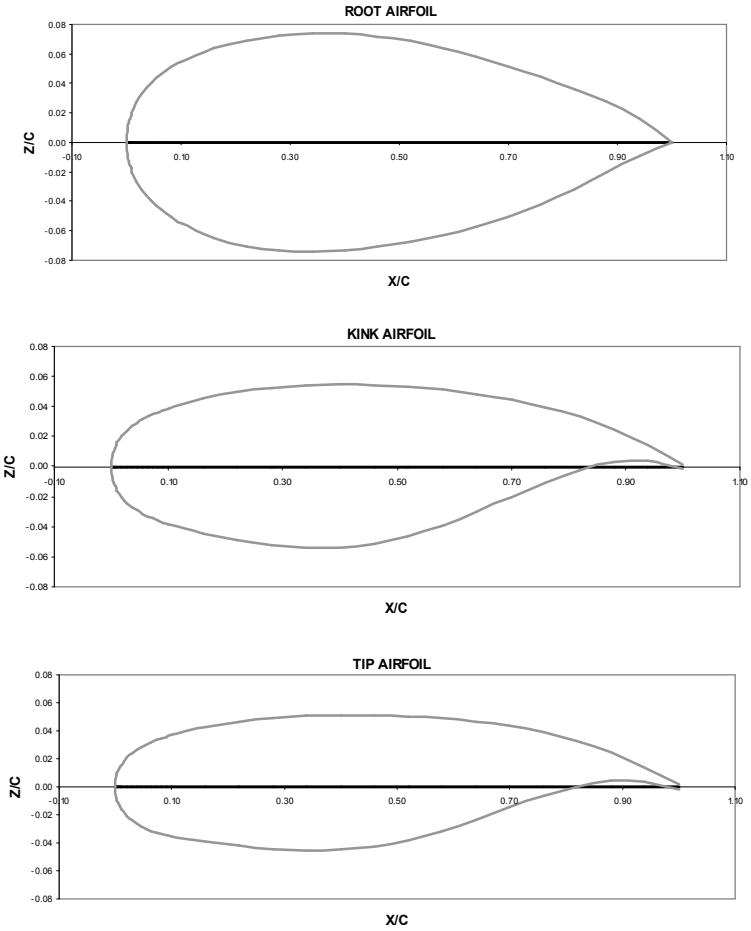

Figure 12 - Airfoil section geometries of the baseline configuration.

Block fuel			11240 kg
MTOW			47784 kg
MUFW			12905 kg
Maximum fuel tank capacity			13984 kg
TOFL			1592 m
HT deflection for trimming at approach			-6.35º
Direct mode	Flight phase B	Natural frequency	2.99 rad/s
		Damping	0.44
	Flight phase C	Natural frequency	1.93 rad/s
		Damping	0.56
SAS	Flight phase B	Natural frequency	3 rad/s
		Damping	0.7
	Flight phase C	Natural frequency	3 rad/s
		Damping:	0.7

Table VIII - Baseline aircraft behavior according to the present formulation.

From **Table VIII** it is possible to check some main performance parameters of the reference aircraft, so that in the optimization, the objective functions and constraints must be chosen in order to select a suitable aircraft relative to some parameters but keeping others at least presenting the same ones as that of the baseline configuration. **Table IX** contains a summary on the run cases objective functions and constraints.

Objective Function	Block Fuel Cruise Mach speed	
Constraints	Fuel tank capacity:	Greater than MUFW
	TOFL:	Less than 1592 m
	HT deflection for trimming at approach:	Less than -6.35º (absolute value)
	Flight quality for flight phase level B:	Greater than acceptable
	Flight quality for flight phase level C:	Greater than poor
	Flight quality with the SAS activated:	Satisfactory

Table IX - Summary on the run cases objective functions and constraints.

5. Results

This section presents the optimization the results of some simulations carried out with the described optimization framework. The workflow engine structure obtained for the all process under consideration can be seen at Figure 13.

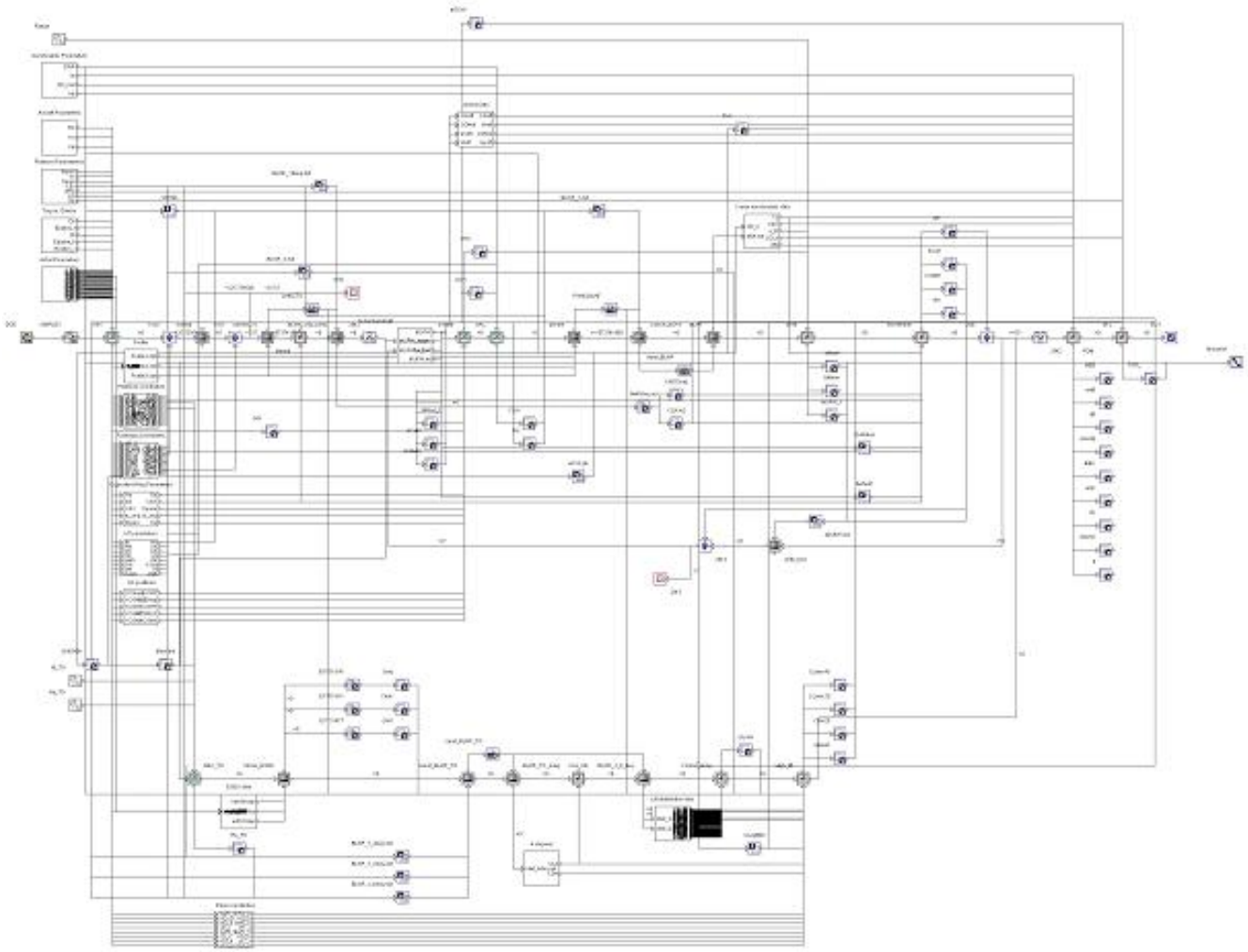

Figure 13 - Workflow engine of the present MDO methodology.

5.1 Case 1

The Test Case I is a single-objective optimization task. In this approach the objective function was composed to minimize the block fuel for a stage length with maximum payload of 2500 nm. The airfoil geometries were not allowed to change in this analysis. For this case a relaxed constrained for the flight quality was adopted. The aircraft will achieve highest flight quality level with the use of stability augmentation system. Fuel volume constraints were also in place for this test case. **Table X** provides a summary of the platform where the case was run. The simplex algorithm does not guarantee that the global maximum or minima point was achieved.

Optimization algorithm	Simplex
Design ID	268
Hardware	AMD Atlhon64 X2 4200, 2GB RAM
Computing time	17 h 59 min

Table X - Optimization performance parameters of the run case 1.

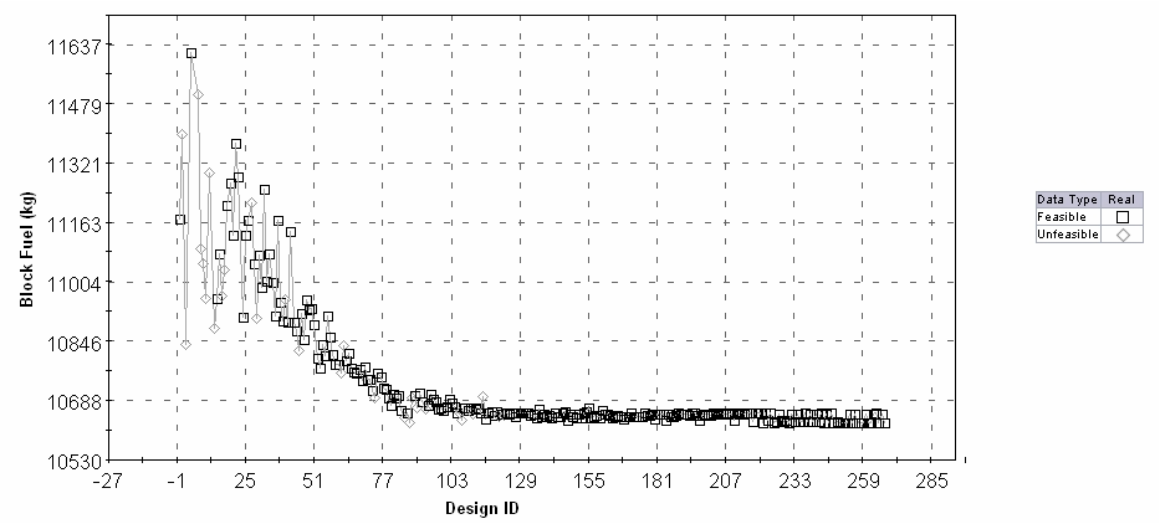

Figure 14: Block fuel history graph for Test Case I.

Leading edge sweep	24.01º
Inner wing taper ratio	0.74
Outer wing taper ratio	0.24
Break station location	31 % of the wingspan
Wing area	104.58 m^2
Wing position (referenced to fuselage length)	43 %
HT volume	1.24
Aspect ratio	10.9

Table XI - Design variables values obtained for Test Case I.

Block fuel:			10629 kg
MTOW:			48727 kg
MUFW:			12294 kg
Maximum fuel tank capacity:			12989 kg
Takeoff field length:			1380 m
HT deflection for trimming at approach:			-5.99º
Direct mode	Flight phase B	Natural frequency:	2.86 rad/s
		Damping:	0.46
	Flight phase C	Natural frequency:	1.84 rad/s
		Damping:	0.58
SAS	Flight phase B	Natural frequency a:	3.00 rad/s
		Damping:	0.7
	Flight phase C	Natural frequency:	3.00 rad/s
		Damping:	0.7

Table XII - Test Case I weights and dynamic behavior.

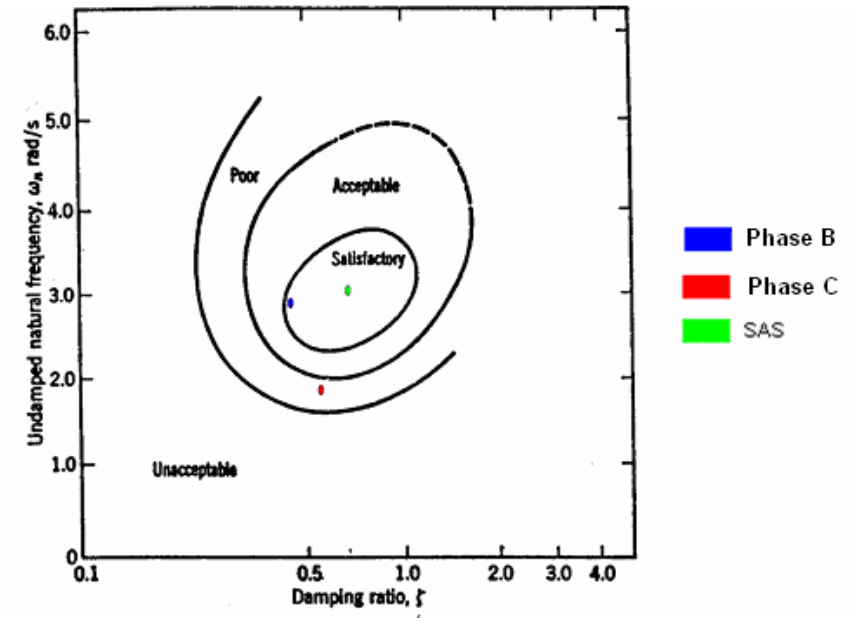

Figure 15 - Flight quality analysis for Test Case I.

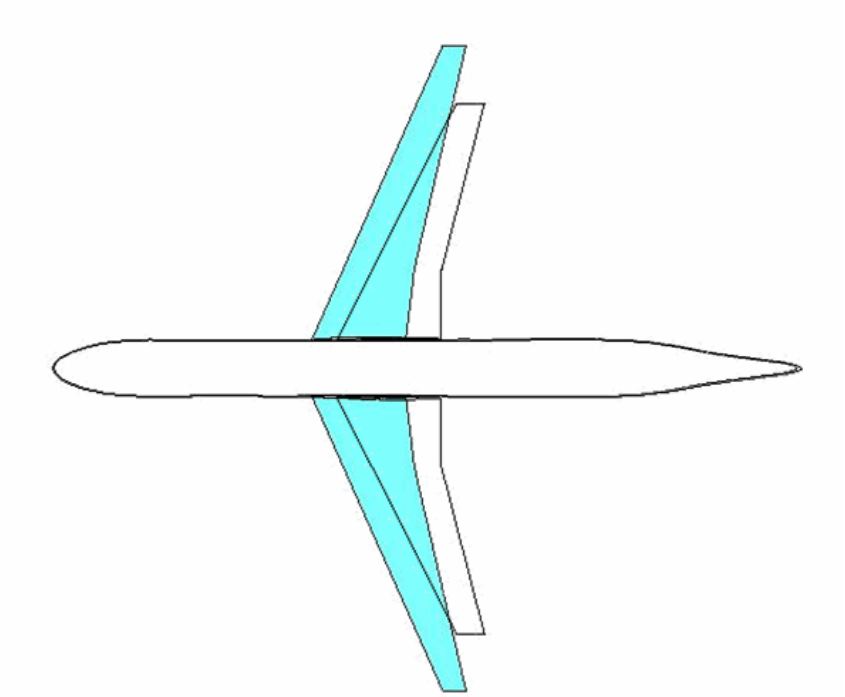

Figure 16 - Baseline aircraft compared to one obtained from Case I (filled in blue color).

5.2 Case II

For this test case II a multi-objective optimization was conducted. The objective functions are related to the block fuel necessary for a 2500-nm mission with maximum payload and the maximum lift coefficient of the configuration. The planform was not allowed to change during the simulation. All airfoils share the same trailing-edge gap. The incidence of the three basic sections – root, break, and tip stations - are optimization variables. The evolutionary algorithm MOGA was employed in the optimization task (**Tab. XIII**).

Optimization algorithm	MOGA
Design ID	2778
Hardware	Pentium 4 - 2.93 GHz - 512 MB de RAM
Computing time	365 h

Table XIII: Optimization performance parameters of the run case 2.

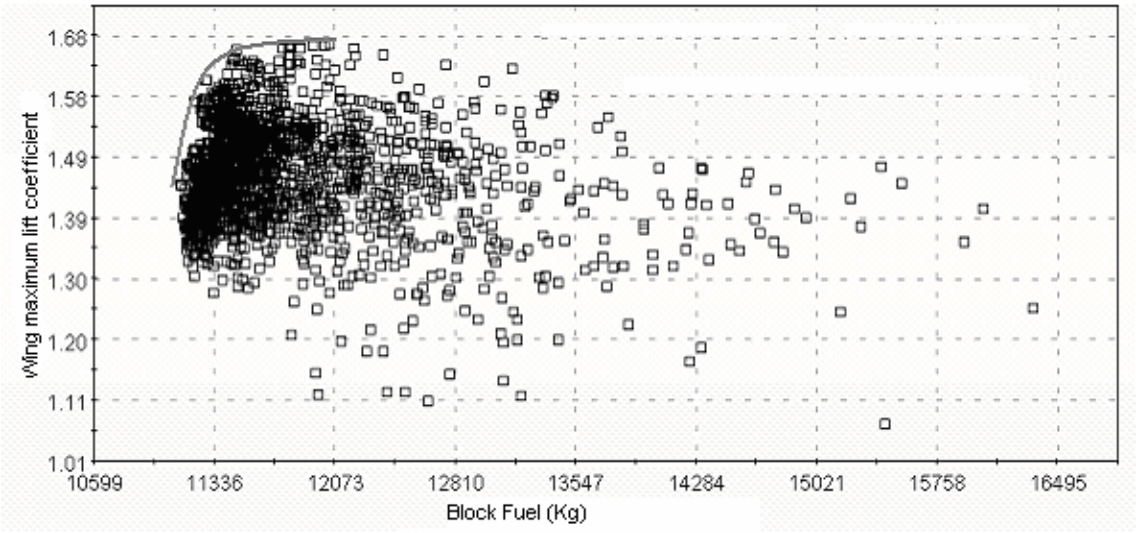

Figure 17 - Pareto Front after 18 generations.

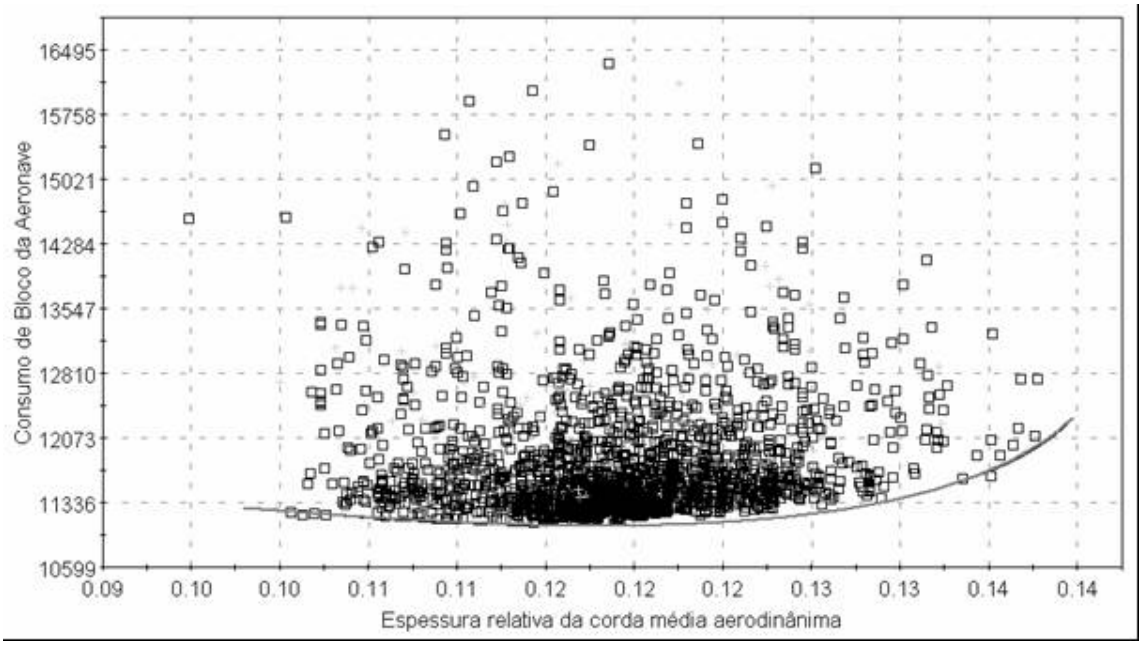

Figure 18 – Relationship between block fuel and maximum thickness of the mean aerodynamic chord.

Each population constituted of 150 individuals. The resulting Pareto Front after 18 generations for the parameters considered in the objective functions can be seen in **Fig. 17**. For the aircraft positioned in the Pareto Front the maximum lift coefficient varies from 1.45 to 1.66 and the block fuel from 11,121 to 12,038 kg. The lowest block fuel consumption occurs for the individuals in Pareto Front presenting 12% of maximum thickness for the section at the mean aerodynamic chord (**Fig. 18**). **Fig. 19** reveals a threshold value laying approximately at 11500 kg for that no increase of C_{Lmax} takes place after increasing the block fuel for the aircraft constituting the Pareto Front. The need for an increased maximum thickness of the airfoil for fuel storage and lowering the wing structural weight causes the degradation in that coefficient. For most aircraft of the Front the stall takes place at outer wing. This is highly undesirable because the loss of roll control in conditions close to stall. Aircraft presenting this kind of behavior can not be certified. In future works a routine to eliminate such configurations during the optimization task will be incorporated into the MDO workflow. **In Fig. 20** the drag divergence of two individuals (no 7 and 14) are compared. The individual presenting the higher C_{Lmax} presents a considerable lower divergence Mach number.

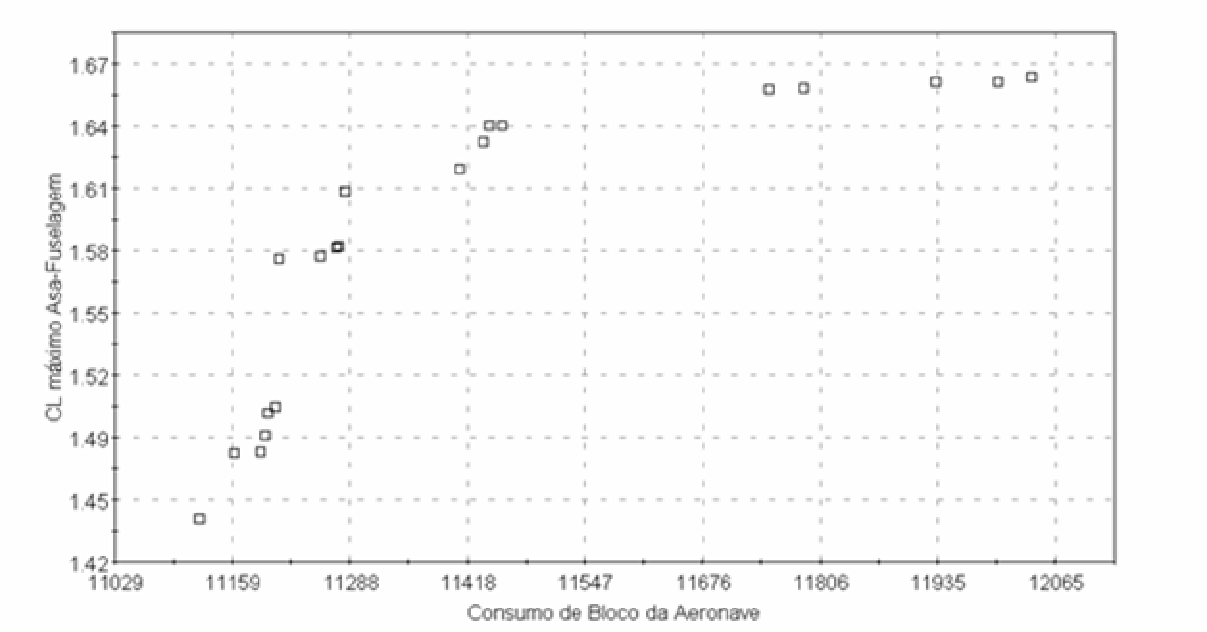

Fig. 19 – Relationship between C_{Lmax} and block fuel for the individuals belonging to Pareto Front.

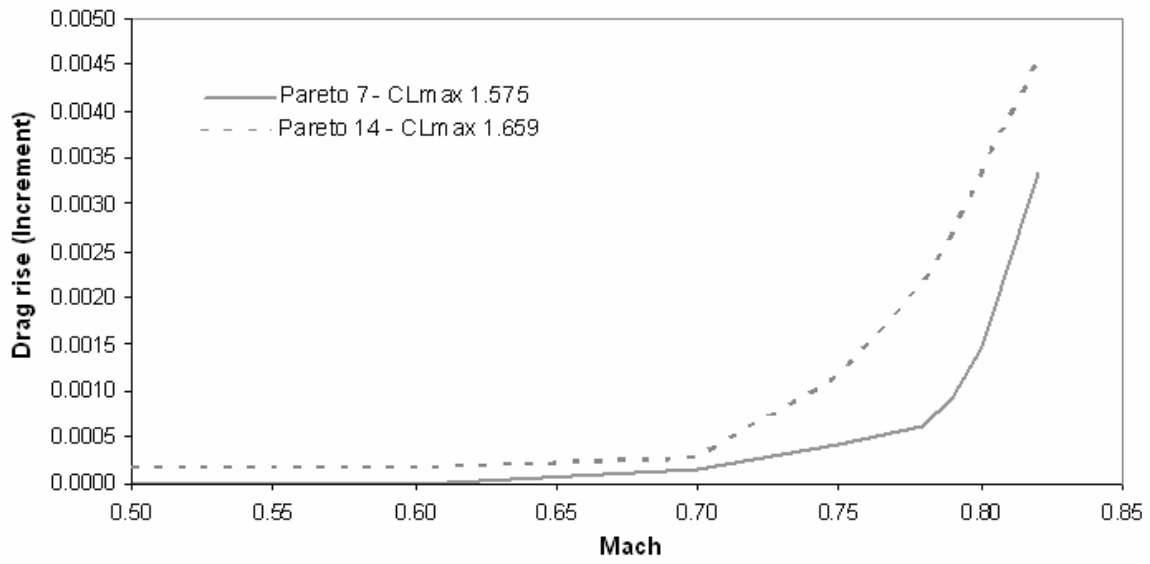

Figure 20 - Drag rise curve for two different individuals of Pareto Front.

6. Concluding Remarks

The simulation reported in the present work revealed that the optimized planform composed of fixed airfoil geometry presented an improvement of 6 % of the block fuel consumption when compared to the baseline configuration. This final configuration has an increased wing weight, which is about 20% heavier than the baseline aircraft. The simulations also indicated that the use of augmentation stability systems can improve the aircraft flight quality in such a way that the wing can be located in a forward position relative to the baseline configuration and the HT volume coefficient becomes therefore lower. This provides lower fuel consumption because the trim and friction drag are reduced for the final configuration. One highlight from the analysis of the simulation was the result concerning the variation of the wing aspect ratio. This parameter reaches the prescribed upper limit and some comments regarding this fact must be enumerated

1) The semi-empirical methods for weight prediction are based on existing aircraft of which there are not enough data for wings with aspect ratios greater than 10. Thus, such methods are not able to predict with reasonable accuracy the wing structural weight of high aspect-ratio wings. Anyway, the wing structural weight of the optimized configuration increased 1500 kg - about 20 % of that calculated for the baseline aircraft. This figure can be considered acceptable.
2) Direct Operational Cost (DOC) is of major importance when designing a transport aircraft. This parameter is composed of several factors such as crew and fuel costs and aircraft acquisition price. It is of widespread knowledge that the acquisition price of the aircraft is proportional to its weight. Therefore, a more fuel efficient aircraft with a very high MTOW might not be equivalent to the aircraft with the minimum DOC.
3) No aeroelastic analysis was performed at the present study. In order to obtain a feasible design this discipline may be part of any MDO workflow and will be taken into account in future work. Flutter and divergence pose an upper limit in the selected wing aspect ratio for a transport aircraft. Active load alleviation and other similar technologies are being employed in order to enable wings with higher aspect ratios.

The simulation for obtaining the optimal airfoil shape is very challenging because of the conflicting requirements of the two objectives, the increase in C_{Lmax} and the reduction of block fuel. Normally higher C_{Lmax} are highly desirable for enabling lower approach and landing speeds, contributing to safety operations, and reducing the wing area in order to fulfill the field performance. However, on the other hand, higher C_{Lmax} may demand more complex flap mechanisms that can lead to a more expensive aircraft and higher maintenance costs. For this reason it seems more suitable to consider the C_{Lmax} requirements as constraints rather than as an objective function.

The simulation revealed that higher incidences of the break station carry for a degradation of the C_{Lmax} of the configuration. However, the block fuel suffers some reduction when that incidence is increased. Increased camber of the tip station airfoil also provides higher C_{Lmax} figures.

The calculation of aerodynamic characteristics such as drag and lift-to-drag ratio is a major factor impacting on higher computing time for any MDO process. Thus, metamodels have to be employed in order to enable reasonable timescales for obtaining optimized configurations. Neural network techniques are the right tool in this direction[10]. Further work will reunite the planform and airfoil design into a single task.

6. Bibliography

1. Isikveren, Askin T., "Quasi-Analytical Modeling and Optimization Techniques for Transport Aircraft Design," Ph.D. Dissertation, Aeronautics Dept.,Royal Institute of Technology, Stockholm, Sweden, 2002.

2. Kroo, I. and Shevell, R., "Aircraft Design: Synthesis and Analysis," Digital Textbook, Desktop Aeronautics, Stanford, CA, 2001.

3. Versiani,, L. C., Paglione, P., and, Mattos, B. S., "Multi-Objective Design Optimization Framework for Conceptual Design of Families of Aircraft**,"** 44th AIAA Aerospace Sciences Meeting and Exhibit, Reno, Nevada, Jan, 9-12, 2006.

4. Torenbeek, E. "*Synthesis of Subsonic Airplane Design"*. S.L.: Kluwer Academic Publishers, 1982.

5. Raymer, D. P. "*Aircraft Design: A Conceptual Approach"*. S.L.: AIAA Educational Series, 2002.

6. Roskam, J. "*Airplane Design*, Part VI – Preliminary Calculation of Aerodynamic", Thrust and Power Characteristics. S.L.: DARCorporation, 2000.

7. Nelson, Robert C. "*Flight Stability and Automatic Control"*. S.L.: McGraw Hill International Editions, 1989.

8. ESDU 76011. *First Approximation to Takeoff Field Length of Multi-Engined Transport Aeroplanes*. Engineering Science Data Unit, 1999.

9. Trépanier, J.Y, Guilbault, F., Ozell, B., and Bouhemdem, D., "A Configurable Framework for Multi-disciplinary Analysis Intergration and Management," Proceedings of the International Council of Aeronautical Sciences (ICAS) 2002 Congress, Toronto, Canada, 2002.

10. Wallach, R., Mattos, B. S., and Girardi, R. M., "Aerodynamic Coefficient Prediction of Transport Aircraft Using Neural Network," 44th AIAA Aerospace Sciences Meeting and Exhibit, Reno, Nevada, Jan, 9-12, 2006.

11. Cavalcanti, J., Mattos, B. S., and Paglione, P., "Optimal Conceptual Design of Transport Aircraft," 11th AIAA Multidisciplinary Analysis and Optimization Conference, Portsmouth, Virginia, Sep, 6-8, 2006.

12. Streshinsky, J. R., Ovcharenko, V. V.. "Aerodynamic Design Transonic Wing Using CFD and Optimization Methods". ANTK "Antonov", Kiev, Ukraine, 1994.

13. ESDU 84026. Aerofoil Maximum Lift Coefficient for Mach Numbers up to 0.4. Engineering Science Data Unit, 1999.

7. Copyright notice